TRAJECTORY SURFACES
OF FRAMED CURVATURE FLOW

Jiří Minarčík & Michal Beneš

Abstract

This work introduces the framed curvature flow, a generalization of both the curve shortening flow and the vortex filament equation. Here, the magnitude of the velocity vector is still determined by the curvature, but its direction is given by an associated time-dependent moving frame. After establishing local existence and global estimates, we analyze the trajectory surfaces generated by different variations of this flow, specifically those leading to surfaces of constant mean or Gaussian curvature.

Contents

1. Introduction

Curvature driven geometric flows have been extensively studied for their favorable properties and various applications across multiple pure and applied fields. We aim to take advantage of these benefits by keeping the magnitude of the local velocity equal to curvature, but at the same time expand and generalise this family of flows by letting the velocity direction be dictated by an associated time-dependent moving frame. We refer to this new class of geometric flows as the *framed curvature flow*.

Although our formulation is based on the Frenet frame, the velocity vector is well defined even in the presence of vanishing curvature, where the normal and binormal vectors are undefined. In the language of Definition 2.2 from [63], the framed curvature flow is not a Frenet frame dependent geometric flow. In this way, it is a modification of the minimal surface generating flow from [64], which is defined only when the torsion and curvature are positive along the whole curve. Another advantage over [64] is the rich configuration space enabled by the additional degrees of freedom from the moving the velocity direction field. To demonstrate the expressivity of this approach we derive variation of the flow that trace out various surfaces of interest in the latter part of the paper.

In this work, we formulate the coupled dynamics of the moving frame and the curvature driven motion, establish local existence and uniqueness for a simplified case of this motion law, provide useful global estimates for geometric and topological quantities, classify possible singularities formed during the flow and analyse generated trajectory surfaces.

The paper is organised as follows: Section 1 introduces the framed curvature flow and prepares the notation and lemmas required for further analysis of the flow and the trajectory surfaces it produces. The analysis is divided into Sections 2 and 3. While the former deals with local behaviour including the local existence and formation of singularities, the latter (Section 3) focuses on long-term behaviour by means of length and area estimates and explores the effects of the moving frame topology. Section 4 then showcases interesting examples of flows from the configuration space of the framed curvature flow framework. Specifically, we explore flows leading to trajectory surfaces of constant mean and Gaussian curvature.

1.1. Motivation. A surprising number of natural and artificial phenomena can be modeled by a one-dimensional filament in three-dimensional Euclidean space, moving according to laws expressed as partial differential equations that depend on both the environment and the shape of the filament. Simplifying complex three-dimensional dynamical systems into a moving space curve allows for faster and more scalable numerical simulations, often revealing new insights and intuitive explanations.

Examples of natural phenomena described via motion laws of space curves include the dynamics of dislocation loops in crystalline materials [65, 48], the motion of scroll waves in excitable media [44, 58], evolution of vortex filaments in liquids via the localized induction approximation [76] or quantum vortices in superfluid media using the Gross–Pitaevskii equation [87, 14].

Evolving space curves can be used for modeling the motion of magnetic field lines in the solar corona [83, 70], the dynamics of elastic rods to model hair

strands in graphics [**17**, **15**] or defects in smectic liquid crystals [**56**]. Geometric flows of curves have also been applied in the context of image processing [**77**], quantum field theory [**12**], origami folding [**27**, **30**], cellular automata [**24**], architecture [**75**], and medicine [**61**].

A significant subset of classical geometric flows can be formulated as a gradient flow of a suitable geometric energy functional [**46**]. Most important example is the mean curvature flow, or curve shortening flow, which minimizes area, or length. It is useful to consider geometric motion laws defined as gradient flow of various other functionals. For instance, one can use the Möbius energy or other O'Hara type energies to find optimal embedings of knots [**19**, **38**, **2**]. Repulsive energies, such as the tangent point energy, can be used in numerous applications in computational geometry and computer graphics [**84**, **85**]. Elastic energies for curves lead to elasticae curves and the Willmore energy for surfaces has been used for finding the optimal torus shape, named Clifford torus [**57**], and can lead to visualy appealing solutions for the sphere eversion problem by starting the evolution from the half-way models such as the Boy's surface. Furthermore, the optimal shapes with respect to the Willmore energy with additional constraints due to Canham and Helfrich leads to shapes of biological membranes found in nature [**21**].

Besides the applications in science and engineering, various geometric flows have proven to be remarkably useful tools in theoretical fields ranging from geometrical measure theory to differential topology, enabling the proofs of many long-standing problems. This includes, but is not limited to, the use of the inverse mean curvature flow for the proof of the Penrose inequality in [**41**] or the Perelman's work on Ricci flow with surgeries [**71**, **72**] leading to the proof of Poincare and Geometrization conjecture. Or more recent work on Ricci flow leading to results such as the Generalized Smale conjecture [**13**] and the Differentiable Sphere Theorem [**22**]. This area is still ripe for new results, particularly in the case of higher codimension motion, which typically receives less attention. For example, open problems from [**32**] may be within the reach, provided that further analysis of framed curvature flow is pursued.

1.2. Framed Curvature Flow. Consider a family of closed curves $\{\Gamma_t\}_{t \in [0, \underline{t})}$ evolving in the time interval $[0, \underline{t})$, where $\underline{t} > 0$ is the terminal time. For a given time $t \in [0, \underline{t})$, the curve Γ_t is represented by a parametrization $\gamma(t, \cdot) \colon S^1 \to \mathbb{R}^3$, where $S^1 = \mathbb{R}/2\pi\mathbb{Z}$ is the unit circle. We use the standard Frenet frame notation, where T, N, and B denote the tangent, normal, and binormal vectors, respectively. The curvature and torsion, given by the Frenet-Serret formulae, are denoted by κ and τ, respectively. Furthermore, $g := \|\partial_u \gamma\|$ is the local rate of parametrization and $\mathrm{d}s = g\,\mathrm{d}u$ is the arclength element.

There are many ways to frame a curve [**18**]. The Frenet frame is in some sense canonical and easy to work with, but is ill-defined at points of vanishing curvature. We define a time-dependent moving frame that is derived from the Frenet frame using an angle functional θ. The normal vector associated with this moving frame will determine the direction of the velocity vector during the framed curvature flow.

Definition 1 (θ-frame)**.** *For an evolving curve* $\{\Gamma_t\}_{t \in [0, \underline{t})}$ *and a functional*
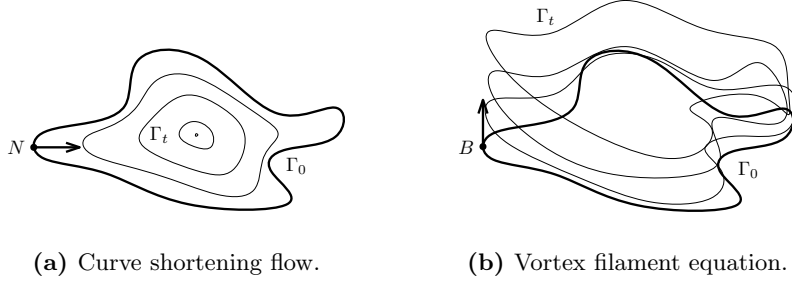$$\theta \in \mathcal{C}^{1,2}([0, \underline{t}) \times S^1; S^1),$$

(a) Curve shortening flow.   **(b)** Vortex filament equation.

Figure 1. Classical examples of space curve motion laws.

we define a θ-frame of Γ_t, with θ-normal ν_θ and θ-binormal β_θ, using a one-parameter group of rotation $\{\mathscr{R}_\theta\}$, as

$$\begin{bmatrix} \nu_\theta \\ \beta_\theta \end{bmatrix} = \mathscr{R}_\theta \begin{bmatrix} N \\ B \end{bmatrix}, \; \text{where } \mathscr{R}_\theta := \begin{bmatrix} \cos\theta & \sin\theta \\ -\sin\theta & \cos\theta \end{bmatrix} \in \mathrm{SO}(2).$$

We denote the moving framed curves as $\{(\Gamma_t, \theta_t)\}_{t\in[0,\underline{t})}$, where $\theta_t := \theta(t, \cdot)$.

Note that $\beta_\theta = T \times \nu_\theta$ and Frenet-Serret type formulae for the θ-frame read

$$\partial_s \begin{bmatrix} T \\ \nu_\theta \\ \beta_\theta \end{bmatrix} = \begin{bmatrix} 0 & \psi_1 & -\psi_2 \\ -\psi_1 & 0 & \psi_3 \\ \psi_2 & -\psi_3 & 0 \end{bmatrix} \begin{bmatrix} T \\ \nu_\theta \\ \beta_\theta \end{bmatrix}, \qquad \begin{aligned} \psi_1 &:= \kappa\cos\theta, \\ \psi_2 &:= \kappa\sin\theta, \\ \psi_3 &:= \tau + \partial_s\theta. \end{aligned}$$

In the context of the trajectory surface defined in Subsection 1.3, ψ_1 and ψ_2 can be interpreted as the geodesic and normal curvatures of Γ_t immersed in Σ_t, respectively. Hereafter, we refer to ψ_3 as the generalised torsion.

Definition 2 (Framed curvature flow). *The family of evolving framed curves* $\{(\Gamma_t, \theta_t)\}_{t\in[0,\underline{t})}$ *is a solution to the* framed curvature flow *if the parametrization* γ *and the angle functional* θ *satisfy the following initial-value problem*

(1a) $\partial_t\gamma = \kappa\nu_\theta \qquad\qquad \partial_t\theta = \upsilon_\theta \qquad\qquad$ *in* $[0,\underline{t}) \times S^1$,

(1b) $\gamma|_{t=0} = \gamma_0 \qquad\qquad \theta|_{t=0} = \theta_0 \qquad\qquad$ *in* S^1,

where γ_0 *and* θ_0 *are the initial conditions and the* θ*-velocity*

$$\upsilon_\theta \in \mathcal{C}^1([0,\underline{t}) \times S^1; \mathbb{R})$$

will be specified later in Subsections 2.3, 4.1 *and* 4.2.

Example 1. *The framed curvature flow subsumes the following classical geometric flows, depicted in Figure* 1, *as its special cases:*
(a) Curve shortening flow *studied e.g. in* [**5, 4**]:
    When $\theta|_{t=0} = 0$ *and* $\upsilon_\theta|_{\theta=0} = 0$, (1) *reduces to* $\partial_t\gamma = \kappa N$.
(b) Vortex filament equation *studied e.g. in* [**76**]:
    When $\theta|_{t=0} = \frac{\pi}{2}$ *and* $\upsilon_\theta|_{\theta=\frac{\pi}{2}} = 0$, (1) *reduces to* $\partial_t\gamma = \kappa B$.
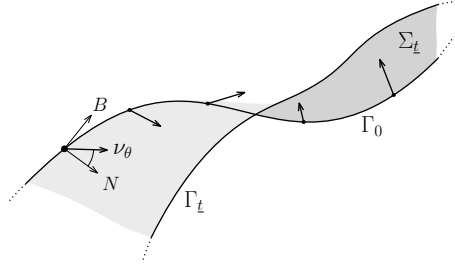
Figure 2. Trajectory surface of a framed curvature flow.

Remark 1. *The framed curvature flow* (1) *can also be viewed as a local harmonic combination of the* curve shortening flow *and the* vortex filament equation *from Examples 1(a) and 1(b), resp. One can also write* (20) *as*

$$\partial_t \gamma = \cos\theta \, \partial_s^2 \gamma + \sin\theta \, \partial_s \gamma \times \partial_s^2 \gamma.$$

This formulation makes clear how the framed curvature flow (1) *is well-defined even when the curvature vanishes and the Frenet frame is undefined.*

Remark 2. *The set of equations* (1) *represents a case of geometric motion with an additional quantity, namely θ, whose velocity depends on the geometry, and vice versa. This kind of coupling has been studied in e.g.* [**69**]*, where the the additional quantity represents the local radius of a bubble vortex tube.*

1.3. Trajectory Surfaces. Similar to how a point mass moving in a homogeneous gravitational field generates a parabola, trajectory surfaces are generated by geometric flows of space curves. As the title suggests, these surfaces are one of the primary concerns of this paper.

We argue that there are two main benefits to examining trajectory surfaces. First, the shape of the trajectory surface encodes the long-term properties of the associated motion law, and thus the knowledge of the generated surfaces may help us understand the overall behaviour of the original geometric flow. Conversely, this framework provides an alternative way to generate and study surfaces with prescribed characteristics, potentially enabling new ways to categorize and understand these surfaces and possibly help tackle various open problems. The formal meaning of trajectory surface is clarified below.

Definition 3 (Trajectory surface, [**64**])**.** *For a given θ-velocity v_θ, terminal time $\underline{t}$ and initial curve Γ_0, we formally define the trajectory surface $\Sigma_{\underline{t}}$ as*

$$\Sigma_{\underline{t}} := \bigcup_{t \in [0,\underline{t})} \Gamma_t,$$

i.e. $\Sigma_{\underline{t}}$ is a surface parametrized by $\gamma(t, u)$ for $t \in [0, \underline{t})$ and $u \in S^1$.

Trajectory surfaces have been studied in [**42**] for the special case of inextensible flows, i.e. geometric flows satisfying $\partial_t g = 0$. An important example of such motion law is the vortex filament equation, mentioned in Example 1. Surfaces generated by this motion law, referred to as Hasimoto surfaces, have been previously considered in [**1**].

Closely related to the trajectory surface is the concept of worldsheet from physics. In the context of string theory, particles sweep out worldlines and

strings sweep out worldsheets in Minkowski space. The equations of motion are induced from the Nambu-Goto action or the Polyakov action [**66**, **36**]. In our case, time is not treated as another dimension as in general relativity, but rather as another parameter.

In this paper, we are specifically interested in trajectory surfaces of constant curvature (see Section 4). In light of this, the following lemma states the formulas for mean and Gaussian curvature of surfaces generated by (1).

Lemma 1. *Mean curvature H and Gaussian curvature K of the trajectory surface Σ_t obtained from Γ_t evolving according to (1) can be expressed as*

$$H = -\psi_2 + \chi \text{ and } K = -\psi_3^2 - \psi_2\chi,$$

respectively. The auxiliary variable χ used in the formulae above reads

$$\chi := \frac{v_\theta}{\kappa} + \frac{\kappa\partial_s\psi_3 + 2\partial_s\kappa\psi_3}{\kappa^3}\psi_1 + \frac{\partial_s^2\kappa - \kappa\partial_s\psi_3^2}{\kappa^3}\psi_2.$$

Proof. The first and the second fundamental form I and $\mathbb{II}$ of Σ_t read

$$\mathrm{I} = \begin{bmatrix} \mathscr{E} & \mathscr{F} \\ \mathscr{F} & \mathscr{G} \end{bmatrix} = \begin{bmatrix} g_{uu} & g_{vu} \\ g_{uv} & g_{vv} \end{bmatrix} = \begin{bmatrix} g^2 & 0 \\ 0 & \kappa^2 \end{bmatrix}, \qquad \mathbb{II} = \begin{bmatrix} \mathscr{L} & \mathscr{M} \\ \mathscr{M} & \mathscr{N} \end{bmatrix},$$

where (g_{ij}) is the metric tensor of Σ_t, $\mathscr{L} = -g^2\psi_2$, $\mathscr{M} = g\psi_3\kappa$ and

$$\mathscr{N} = \kappa v_\theta + \psi_1 \frac{\kappa\partial_s\psi_3 + 2\partial_s\kappa\psi_3}{\kappa} + \psi_2 \frac{\partial_s^2\kappa - \kappa\psi_3^2}{\kappa}.$$

Finally, the mean curvature H and the Gaussian curvature K are

$$K = \frac{\det \mathbb{II}}{\det \mathrm{I}} = \frac{\mathscr{L}\mathscr{N} - \mathscr{M}^2}{\mathscr{E}\mathscr{G} - \mathscr{F}^2}, \qquad H = \mathrm{tr}\left(\mathbb{II}\left(\mathrm{I}^{-1}\right)\right) = \frac{\mathscr{L}}{\mathscr{E}} + \frac{\mathscr{N}}{\mathscr{G}}.$$

For more details, we refer the reader to Section 2 in [**64**].   q.e.d.

Remark 3. *The principle curvatures of the trajectory surface Σ_t generated during (1) are $\kappa_{1,2} = -\psi_2 + \chi \pm \sqrt{\zeta}$, where $\zeta := \psi_2^2 - \psi_2\chi + \chi^2 + \psi_3^2$ and χ is the auxiliary variable from Lemma 1.*

Further analysis of trajectory surfaces has been recently carried out in [**86**], which includes a description of properties of u-curves, e.i. curves given by $\gamma(\cdot, u)$ with a fixed parameter $u \in S^1$.

2. Local Analysis

This section focuses on local properties, both in time and parameter space, of the solution to the framed curvature flow equation (1). In particular, we state the evolution equations of the local geometric quantities in Subsection 2.1, study the effects of non-trivial tangential redistribution in Subsection 2.2 and with the help of these preliminary results we establish the local existence and uniqueness of the solution in Subsection 2.3. The Subsection 2.4 provides an overview of possible singularities formed during curvature blow-up events.

2.1. Evolution Equations. Evolution equations for local geometric quantities, like the rate of parametrisation, curvature or torsion, during general geometric flows of space curves have been extensively studied in many pieces of literature before. See e.g. [67] for a general algebraic approach or [16] for the treatment of geometric motion law similar to (1). Nevertheless, we state these equations and adopt them for the specific case of framed curvature flow for reader's convenience.

Lemma 2. *The arc-length commutator $[\partial_t, \partial_s]$ during the framed curvature flow* (1) *with the angle functional θ is given by*

$$[\partial_t, \partial_s] := \partial_t \partial_s - \partial_s \partial_t = \kappa^2 \cos\theta \, \partial_s. \tag{2}$$

Equivalently, $\partial_t g = -\kappa^2 \cos\theta \, g = -\kappa\psi_1 g$.

Proof. The statement is a special case of Proposition 1 from [16].   q.e.d.

Lemma 3. *The Frenet frame during the framed curvature flow* (1) *satisfies*

$$\partial_t \begin{bmatrix} T \\ N \\ B \end{bmatrix} = \begin{bmatrix} 0 & \xi_1 & -\xi_2 \\ -\xi_1 & 0 & \xi_3 \\ \xi_2 & -\xi_3 & 0 \end{bmatrix} \begin{bmatrix} T \\ N \\ B \end{bmatrix}, \qquad \begin{aligned} \xi_1 &:= \partial_s \psi_1 - \tau\psi_2, \\ \xi_2 &:= -\partial_s \psi_2 - \tau\psi_1, \\ \xi_3 &:= \kappa^{-1}(\psi_1 \partial_s \tau + \partial_s^2 \psi_2 - \tau^2), \end{aligned}$$

while the evolution of θ-normal ν_θ and θ-binormal β_θ can be expressed as

$$\partial_t \begin{bmatrix} T \\ \nu_\theta \\ \beta_\theta \end{bmatrix} = \begin{bmatrix} 0 & \zeta_1 & -\zeta_2 \\ -\zeta_1 & 0 & \zeta_3 \\ \zeta_2 & -\zeta_3 & 0 \end{bmatrix} \begin{bmatrix} T \\ \nu_\theta \\ \beta_\theta \end{bmatrix}, \qquad \begin{aligned} \zeta_1 &:= \partial_s \kappa, \\ \zeta_2 &:= -\psi_3 \kappa, \\ \zeta_3 &:= \upsilon_\theta + \xi_3. \end{aligned}$$

Finally, the curvature κ and torsion τ evolve as

$$\partial_t \kappa = \kappa^2 \psi_1 + \kappa^{-1}\left(\partial_s^2 \psi_1 - \partial_s \tau\psi_2 - 2\tau\partial_s\psi_2 + \tau\psi_1\right), \tag{3}$$

$$\partial_t \tau = \kappa\psi_1(\tau + \psi_3) + \partial_s\left[\kappa^{-2}\left(\partial_s^2 \psi_2 + 2\partial_s\kappa\psi_1\psi_3 - \kappa\psi_2\psi_3 + \kappa\psi_1\partial_s\psi_2\right)\right]. \tag{4}$$

Proof. Proved by substitution to Example 5.7 from [67].   q.e.d.

The evolution equations for the θ-frame local quantities ψ_1, ψ_2 and ψ_3 are more involved, but can be expressed as

$$\begin{aligned} \partial_t \psi_1 &= \partial_t \kappa \cos\theta - \psi_2 \upsilon_\theta, \\ \partial_t \psi_2 &= \partial_t \kappa \sin\theta + \psi_1 \upsilon_\theta, \\ \partial_t \psi_3 &= \partial_t \tau + \partial_s \upsilon_\theta + \kappa\psi_1\partial_s\theta, \end{aligned}$$

where $\partial_t \kappa$ and $\partial_t \tau$ shall be substituted from (3) and (4).

2.2. Tangential Redistribution. To simplify previous calculations, we ignored the tangential velocity in (1) by setting $v_T := \langle \partial_t \gamma, T \rangle = 0$. Apart from advection of the θ-frame along the curve, this choice does not affect the geometry of the moving curve. Non-trivial tangential velocity can, however, be useful for improving numerical stability and existence analysis. We wish to do the latter in the following subsection. Hence we introduce and analyse appropriate tangential term here. Specifically, we use the tangential velocity term developed and used in [40, 47, 60] and modify it for our motion law in the following lemma.

Lemma 4. *Assume that for all $t \in [0, \underline{t})$ and all $s \in \mathbb{R}/L(\Gamma_t)\mathbb{Z}$ the tangential velocity v_T satisfies the following integro-differential equation*

$$(5) \qquad v_T(t,s) = v_{T,0}(t) + \int_0^s \kappa \psi_1 \, \mathrm{d}\overline{s} - \frac{s}{L(\Gamma_t)} \int_{\Gamma_t} \kappa \psi_1 \, \mathrm{d}\overline{s},$$

where $v_{T,0}(t) = v_T(t, 0)$ is any differentiable function $v_{T,0} \in \mathcal{C}^1([0, \underline{t}))$. Then the quantity $L(\Gamma_t)^{-1}g$ is constant during the framed curvature flow (1).

Proof. With $\partial_t \gamma = \kappa \nu_\theta + v_T T$, the arc-length commutator from Lemma 2 is

$$[\partial_t, \partial_s] = (\kappa \psi_1 - \partial_s v_T)\partial_s$$

and we have $\partial_t g = (-\kappa \psi_1 + \partial_s v_T)g$. Note that the choice of v_T does not affect the evolution of length $L(\Gamma_t)$, provided the curves Γ_t are closed. And thus

$$\partial_t \left(\frac{g}{L(\Gamma_t)} \right) = \frac{g}{L(\Gamma_t)^2} \left[(-\kappa \psi_1 + \partial_s v_T) L(\Gamma_t) + \int_{\Gamma_t} \kappa \psi_1 \, \mathrm{d}s \right].$$

Substitution of $\partial_s v_T$ from (5) yields the vanishing right-hand side.   q.e.d.

With a suitable choice of parametrization and the tangential velocity satisfying (5) we can achieve uniform parametrization throught the flow.

Proposition 1. *Assume that the initial curve Γ_0 is uniformly parametrized such that $g(0, u) = L(\Gamma_0)$ for all $u \in S^1$. Let $\{(\Gamma_t, \theta_t)\}_{t \in [0, \underline{t})}$ be a solution to the framed curvature flow with tangential velocity* (5). *Then the curve Γ_t is parametrized uniformly during the whole flow, i.e. $g(t, u) = L(\Gamma_t)$ for all $t \in [0, \underline{t})$ and $u \in S^1$.*

Proof. Straightforward application of Lemma 4.   q.e.d.

Note that v_T in (5) is indeed well defined on the periodic domain as one can easy verify that $v_T|_{s=0} \equiv v_T|_{s=L(\Gamma_t)}$ and $\partial_s v_T|_{s=0} \equiv \partial_s v_T|_{s=L(\Gamma_t)}$.

2.3. Local Existence. This subsection establishes local existence and uniqueness for the framed curvature flow constrained by assumptions outlined in Lemma 5 or Lemma 6. First, it is important to note that the right-hand side of (1) is well-defined even in the absence of the Frenet frame (see Remark 1).

The existence result is achieved by extending the method of abstract theory of analytic semi-flows in Banach spaces from [**74**, **9**, **10**, **55**]. In particular we formulate (1) in terms of an extended four-dimensional system by treating θ as another dimension, and follow the existence proof of a similar system of equations from [**16**]. First, let $\hat{\gamma} \colon [0, \underline{t}) \times S^1 \to \mathbb{R}^4$ denote the extended parametrization $\hat{\gamma} := [\gamma_1, \gamma_2, \gamma_3, \theta]^T$. And consider the extended system

$$(6) \qquad\qquad \partial_t \hat{\gamma} = \hat{\mathcal{A}} \partial_s^2 \hat{\gamma} + f(\partial_s \hat{\gamma}, \hat{\gamma}),$$

where $f \in \mathcal{C}(\mathbb{R}^{4,4}; \mathbb{R}^4)$ and the principal part of the right-hand side reads

$$\hat{\mathcal{A}} = \left[\begin{array}{c|c} \mathcal{A} & 0 \\ \hline \beta^T & \alpha \end{array} \right], \quad \mathcal{A} = \cos\theta\, \mathbb{I} + \sin\theta\, [T]_\times = \left[\begin{array}{ccc} \cos\theta & -\sin\theta\, T_3 & \sin\theta\, T_2 \\ \sin\theta\, T_3 & \cos\theta & -\sin\theta\, T_1 \\ -\sin\theta\, T_2 & \sin\theta\, T_1 & \cos\theta \end{array} \right],$$

where $\mathbb{I}_{ij} = \delta_{ij}$, $([T]_\times)_{ij} = \sum_k \varepsilon_{ijk} T_k$ for $i, j \in \{1, 2, 3\}$, and $\alpha \in \mathbb{R}^+$, $\beta \in \mathbb{R}^3$ are fixed parameters of the framed curvature flow (1) with the following θ-velocity

$$(7) \qquad\qquad v_\theta = \alpha \partial_s^2 \theta + \kappa \langle \beta, N \rangle + f_4(\partial_s \hat{\gamma}, \hat{\gamma}).$$

We want the system (6) to be parabolic. As the spectrum of $\hat{\mathcal{A}}$ is

$$\sigma(\hat{\mathcal{A}}) = \sigma(\mathcal{A}) \cup \{\alpha\} = \{\alpha, \cos\theta, e^{\pm i\theta}\},$$

the eigenvalues α and $\cos\theta$ must be positive. In order to proceed towards the local existence result, additional constraints have to be laid down to ensure that this property is guaranteed. In the following lemmas, we provide two different ways to achieve this goal.

Lemma 5. *Let $\beta = 0$ and $\alpha > 0$ be fixed parameters of the extended system of equations (6) with $f_4 \equiv 0$ and assume that θ_0 satisfies $|\theta(0, u)| < \frac{\pi}{2}$ for all $u \in S^1$. Then any solution $\{(\Gamma_t, \theta_t)\}_{t \in [0,\underline{t}]}$ to (1) will satisfy $|\theta| < \frac{\pi}{2}$ everywhere and the extended system (6) will remain parabolic.*

Proof. The statement is a consequence of the weak maximum principle for the angle functional θ. Using the notation from Chapter 7.1.4 of [**28**], we have

$$(8) \qquad \partial_t\theta + \mathcal{L}\theta = 0,$$

where $\mathcal{L} := -\alpha\partial_s^2 = -\alpha g^{-2}\partial_u^2 + \alpha g^{-3}\partial_u g\partial_u$. Thanks to the trivial right-hand side of (8), we can use Theorem 8 from Chapter 7 of [**28**] and conclude that

$$|\theta(t, u)| \leqslant \max_{\overline{u} \in S^1} |\theta(0, \overline{u})| < \frac{\pi}{2}$$

for all $(t, u) \in [0, \underline{t}] \times S^1$. The last inequality holds due to assumptions. q.e.d.

Introducing additional assumptions on the curvature allows us to extend the result from Lemma 5 for the case of non-trivial β and f_4 from (7).

Lemma 6. *Assume $|\theta_0| < \frac{\pi}{2}$ on S^1 and there exist $C_1, C_2 > 0$ such that for all $u \in S^1$ and all $t \in [0, \underline{t}]$ we have $\kappa(t, u) \leqslant C_1$ and $f_4(t, u) \leqslant C_2$, where*

$$\underline{t} := \frac{1}{C_1|\beta| + C_2} \left(\frac{\pi}{2} - \max_{u \in S^1} |\theta_0(u)| \right).$$

Then $|\theta| < \frac{\pi}{2}$ holds everywhere on $[0, \underline{t}] \times S^1$ and (6) remains parabolic.

Proof. The non-difusive term $v_\theta - \alpha\partial_s^2\theta$ of the equation (7) is bounded as

$$|v_\theta - \alpha\partial_s^2\theta| \leqslant C_3,$$

where $C_3 := C_1|\beta| + C_2$ is a positive constant. Using this value we construct

$$\theta_- := \min_{u \in S^1} |\theta_0(u)| - C_3, \qquad \theta_+ := \max_{u \in S^1} |\theta_0(u)| + C_3,$$

which are subsolution and supersolution to θ (see Lemma 5). Since $|\theta_\pm|$ stays bellow $\frac{\pi}{2}$ for all $t \in [0, \underline{t}]$, we concur that $|\theta|$ is bounded by $\frac{\pi}{2}$ as well. q.e.d.

To prepare for the existence proof, further notation needs to be introduced. For any $\varepsilon \in (0, 1)$ and any $k \in \{0, \frac{1}{2}, 1\}$ we define the following family of Banach spaces of Hölder continuous functions

$$\mathcal{E}_k := h^{2k+\varepsilon}(S^1) \times h^{2k+\varepsilon}(S^1) \times h^{2k+\varepsilon}(S^1) \times h^{2k+\varepsilon}(S^1),$$

where $h^{2k+\varepsilon}(S^1)$ is a little Hölder space (see Section 4.1 in [**16**]). With the aid of the previous lemmas and the appropriate tangential velocity term described in Subsection 2.2, we can now state the local existence result.

Proposition 2. *Consider* (1) *with additional tangential velocity satisfying* (5) *from in Subsection* 2.2 *and assume that*

(a) *the initial extended parametrization* $\hat{\gamma}|_{t=0}$ *belongs to* $\mathcal{E}_1$,
(b) *the initial parametrization* γ_0 *satisfies* $\|\partial_u \gamma_0\| = L(\Gamma_0)$ *on* S^1,
(c) *f is* $\mathcal{C}^2$ *smooth and globally Lipschitz continuous,*
(d) *the assumptions of Lemma* 5 *or Lemma* 6 *are satisfied.*

Then there exists $\underline{t} > 0$ *and a unique family of framed curves* $\{(\Gamma_t, \theta_t)\}_{t \in [0, \underline{t})}$ *satisfying* (6) *with tangential velocity* (5) *such that* $\hat{\gamma} \in \mathcal{C}([0, \underline{t}); \mathcal{E}_1) \cap \mathcal{C}^1([0, \underline{t}); \mathcal{E}_0)$.

Proof. We extend the proof of Theorem 4.1 from [**16**] to the parametrization with the framing angle $\hat{\gamma}$. We rewrite the extended system (6) as an abstract parabolic equation:

$$(9) \qquad\qquad \partial_t \hat{\gamma} + \mathscr{F}(\hat{\gamma}) = 0$$

for $\hat{\gamma} \in \mathcal{E}_1$, where $\mathscr{F}$ is operator mapping from $\mathcal{E}_1$ to $\mathcal{E}_0$. Using Lemma 2.5 from [**9**] as in the proof of Proposition 4 from [**16**], the Frechet derivative $\mathscr{F}'$ of the operator $\mathscr{F}$ from (9) belongs to the maximum regularity class $\mathcal{M}(\mathcal{E}_1, \mathcal{E}_0)$. The solution $\hat{\gamma}$ exists in

$$\mathcal{C}([0, \overline{t}]; \mathcal{E}_1) \cap \mathcal{C}^1([0, \overline{t}]; \mathcal{E}_0)$$

for any $\overline{t} \in (0, \underline{t})$ due to Theorem 2.7 from [**9**].   q.e.d.

For more details, we refer the reader to [**16**] or to the original literature [**74**, **9**, **10**, **55**] of the abstract theory of analytic semi-flows in Banach spaces.

Proposition 3. *Let the assumptions of Proposition* 2 *hold and suppose that the maximal time of existence* $\underline{t}$ *is finite, then*

$$\limsup_{t \to \underline{t}} \max_{u \in S^1} \kappa(t, u) = +\infty \quad \vee \quad \limsup_{t \to \underline{t}} \max_{u \in S^1} |\partial_s^2 \theta(t, u)| = +\infty.$$

Proof. For contradiction, assume that the maximal time of the existence $\underline{t}$ is finite and that both κ and $|\partial_s^2 \theta|$ are bounded. Since the assumptions of Proposition 2 are satisfied, the solution $\hat{\gamma}$ belongs to $\mathcal{C}([0, \overline{t}]; \mathcal{E}_1) \cap \mathcal{C}^1([0, \overline{t}]; \mathcal{E}_0)$ for any $\overline{t} \in (0, \underline{t})$. Moreover, $\partial_s^2 \hat{\gamma}$ is bounded by the assumptions because

$$\|\partial_s^2 \hat{\gamma}\|^2 = \|\partial_s^2 \gamma\|^2 + |\partial_s^2 \theta|^2 = \kappa^2 + |\partial_s^2 \theta|^2.$$

Thus, by the maximum regularity, the extended solution $\hat{\gamma}$ belongs to the space $\mathcal{C}([0, \underline{t}]; \mathcal{E}_1) \cap \mathcal{C}^1([0, \underline{t}]; \mathcal{E}_0)$ and can be continued beyond $[0, \underline{t})$, which contradicts the maximal time assumption. More details can be retrieved from the last part of Theorem 4.1 from [**16**].   q.e.d.

The behaviour of Γ_t during the curvature blow-up event described in Proposition 3 is detailed in the next subsection.

2.4. Formation of Singularities.
The expressive power of the framed curvature flow framework allows for the occurrence of unusual singularity types during curvature blow-up events. In general, understanding these singularities has been crucial for analyzing the behavior of various geometric flows. For our work, it will be particularly important for the global analysis in Section 3.

Singularities of geometric flows have been studied in e.g. [**45**, **25**, **52**, **8**, **43**] or [**5**], where the motion of planar curve has been extended beyond curvature
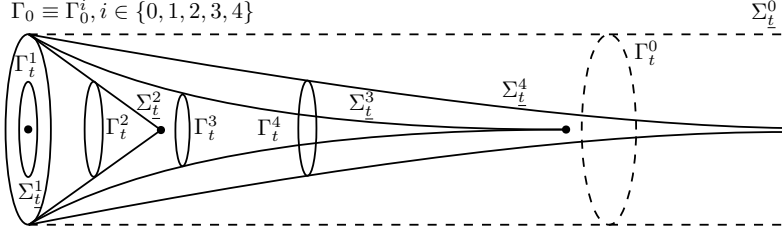
Figure 3. Depiction of singularity typologies from Definition 4 for circular initial condition Γ_0 and uniform theta angle. Upper indices 1 to 4 denote the flat, cone, pinch and infinite pinch scenario, respectively. The dashed line represents the trajectory of the vortex filament equation for reference.

singularities via a higher dimensional flow of an associated space curve. The existence of flows past various singularities has also been addressed by other means such as by using the concept of viscosity solutions for the level-set formulation of curvature driven flows in [**68**, **33**], topological surgeries [**72**] or by analysis of self-similar shrinkers in [**81**].

In [**4**], Altschuler showed that the blow-up limits of space curves under the curve shortening flow are planar. The situation for framed curvature flow is more complicated. The following definition clarifies the meaning of different types of singularities which may occur during (1).

Definition 4 (Singularity typologies). *The event at which the curvature κ approaches infinity at time $\underline{t}$ and $L(\Gamma_t) \to 0$ as t approaches $\underline{t}$ (the curve Γ_t shrinks to a point) during the framed curvature flow* (1) *is called:*

1. *Flat singularity if and only if $\theta_t \rightrightarrows 0$ as t approaches $\underline{t}$.*
   (θ-frame uniformly approaches the Frenet frame).
2. *Cone singularity if and only if $\theta_t \rightrightarrows \Theta \in (-\frac{\pi}{2}, \frac{\pi}{2}) \backslash \{0\}$ as t approaches $\underline{t}$.*
3. *Pinch singularity if and only if $\theta_t \rightrightarrows \Theta \in \{\pm\frac{\pi}{2}\}$ as t approaches $\underline{t}$.*

Furthermore, when the trajectory surface $\Sigma_{\underline{t}}$ is unbounded, the case 3. is called infinite pinch singularity.

The flat singularity occurs in the classical example of curve shortening flow. For the case of simple planar curves, this singularity is guarantied by the Gage-Hamilton-Grayson theorem [**31**, **37**]. Embedded space curves under the curve shortening flow do not necessarily shrink to a point, however the Gage-Hamilton-Grayson theorem can be extended in the case of simple spherical curves [**62**]. Other singularity types from Definition 4 are illustrated in the next set of analytical examples with simple evolution of circle.

Example 2 (Cone singularity). *Let Γ_0 be a circle with radius $\rho_0 > 0$ and consider $v_\theta \equiv 0$ with $\theta_0 \equiv \phi \in (0, \frac{\pi}{2})$. This setup leads to the famous solution for shrinking circle with radius $\rho(t) = (\rho_0^2 - 2t \cos\phi)^{\frac{1}{2}}$ which vanishes at the terminal time $\underline{t} = (2\cos\phi)^{-1}\rho_0^2$. However, due to the non-trivial binormal velocity term $\langle \partial_t \gamma, B \rangle = \kappa \sin\phi \neq 0$, the singularity occurs at a point shifted in*

the binormal direction from the center of the initial circle by a distance

$$\underline{z} = \left(\rho_0 - \left(\rho_0^2 - 2\underline{t}\cos\phi\right)^{\frac{1}{2}}\right)\tan\phi = \rho_0\tan\phi.$$

This leads to a conical trajectory surface with a cone singularity.

Example 3 (Pinch singularity). *Again, consider a circle* Γ_0 *with radius* $\rho_0 > 0$ *and* $\theta_0 \equiv \phi \in (0, \frac{\pi}{2})$. *To illustrate the pinch singularity, let*

$$\partial_t\theta = \frac{\tan\theta - 2\kappa\sqrt{\underline{t} - t}}{2(\underline{t} - t)},$$

where $\underline{t} = (\sin\phi)^{-2}\rho_0$. *This* θ-*velocity is constructed so that* $\rho = \sin\theta\sqrt{\underline{t} - t}$ *and* $\partial_t z = \kappa\sin\theta = \sqrt{\underline{t} - t}$. *Even though the time derivative of the shift distance z diverges as t approaches* $\underline{t}$, *its definite integral remains finite:*

$$\lim_{t\to\underline{t}} z(t) = \lim_{t\to\underline{t}} \int_0^t \frac{1}{\sqrt{\underline{t} - \bar{t}}}\,\mathrm{d}\bar{t} = \lim_{t\to\underline{t}} \left[-2\sqrt{\underline{t} - \bar{t}}\right]_{\bar{t}=0}^{\bar{t}=t} = 2\sqrt{\underline{t}}.$$

The pinch singularity thus develops at a point located at a $2\sqrt{\underline{t}}$ *distance form the center of the original circle.*

Example 4 (Infinite pinch singularity). *With the same setup of initial conditions as in the previous examples, we now consider* $\partial_t\theta = 2\rho_0^{-2}$. *This velocity leads to* $\theta(t) = 2t\rho_0^{-2}$ *and* $\rho(t) = \rho_0(1 - \sin(2\rho_0^{-1}t))^{\frac{1}{2}}$. *Thus the circle shrinks to a point at the time* $\underline{t} = \frac{1}{4}\pi\rho_0^2$ *and*

$$(10) \qquad \partial_t z = \rho^{-1}\sin(2\rho_0^{-1}t)) = \rho_0^{-1}(1 - \sin(2\rho_0^{-1}t)))^{-\frac{1}{2}}\sin(2\rho_0^{-1}t)).$$

Unlike in the Example 3, the integral of (10) *diverges and thus the infinite pinch singularity is formed.*

All singularity typologies from Examples 2, 3 and 4 are depicted in Figure 3.

Remark 4. *Let us recall the definition of type-I and type-II singularity, studied in e.g.* [**45**, **25**, **52**]. *This classification of curvature blow-up events is based on the comparison of the curvature growth near* $\underline{t}$ *with the function* $(\underline{t} - t)^{\frac{1}{2}}$. *Formally, a blow-up singularity is classified as type-I if*

$$(11) \qquad \lim_{t\to\underline{t}} M_t(\underline{t} - t) := \lim_{t\to\underline{t}}[\max_{u\in S^1}\kappa^2(t, u)](\underline{t} - t)$$

is bounded, and as type-II otherwise. In terms of this classical notation, the singularities from Example 2 and 3 are type-I:

- *In Example 2, we have* $M_t = \rho^{-2}(t) = (\rho_0^2 - 2t\cos\phi)^{-1} = 2\cos\phi(\underline{t}-t)^{-1}$, *where the terminal time is* $\underline{t} = (2\cos\phi)^{-1}\rho_0^2$. *Thus*

$$\lim_{t\to\underline{t}} M_t(\underline{t} - t) = 2\cos\phi < +\infty.$$

- *Similarly in Example 3, the radius reads* $\rho = (\underline{t} - t)^{\frac{1}{2}}\sin\theta$ *and therefore*

$$\lim_{t\to\underline{t}} M_t(\underline{t} - t) = \lim_{t\to\underline{t}}\max_{u\in S^1}(\sin\theta_t(u))^{-2} = 1 < +\infty.$$

Whereas the infinite pinch singularity from Example 4 is type-II:

- *Since in Example 4, the radius is* $\rho(t) = \rho_0(1 - \sin(2\rho_0^{-1}t))^{-\frac{1}{2}}$, *the term* M_t *behaves as* $(\underline{t} - t)^2$ *near* $\underline{t}$ *and the limit* (11) *diverges.*

Further analysis of these connections is left for a future work.

The study of singularity formation is an extensive field of research, and this subsection offers only a brief exploration of potential blow-up scenarios within the context of the recently introduced framed curvature flow. Future work can involve for instance the analysis of singularity profiles leading to the self-shrinking Abresch–Langer curves [3].

3. Global Analysis

This section examines the global aspects of solutions to the framed curvature flow, with an emphasis on the properties of global geometric quantities and their long-term behavior. Subsection 3.1 provides several global estimates for the length and generated surface area, Subsection 3.2 explores the evolution of the largest projected algebraic area, and Subsection 3.3 presents selected key facts related to the topology of the θ-framing.

3.1. Global Estimates. We aim to derive useful estimates for global geometric quantities such as length and generated area. To this end, we first establish evolution equations for these quantities and then state the assumptions on which the subsequent bounds in this subsection are based.

Lemma 7. *The evolution of the length $L(\Gamma_t)$ of the curve Γ_t and the total area $A(\Sigma_t)$ of the trajectory surface Σ_t during (1) is*

$$(12) \qquad \frac{\mathrm{d}}{\mathrm{d}t} L(\Gamma_t) = - \int_{\Gamma_t} \kappa \psi_1 \, \mathrm{d}s, \qquad \frac{\mathrm{d}}{\mathrm{d}t} A(\Sigma_t) = \int_{\Gamma_t} \kappa \, \mathrm{d}s.$$

Proof. The first part of (12) is due to (2), the second one follows from

$$\frac{\mathrm{d}}{\mathrm{d}t} \int_{\Sigma_t} \mathrm{d}A = \frac{\mathrm{d}}{\mathrm{d}t} \int_0^t \int_{\Gamma_{\bar{t}}} \kappa \, \mathrm{d}s \, \mathrm{d}\bar{t},$$

where $\mathrm{d}A$ is obtained from $\mathscr{E} = g^2$, $\mathscr{F} = 0$ and $\mathscr{G} = \beta^2 + \gamma^2 = \kappa^2$ as

$$\mathrm{d}A = \sqrt{\mathscr{E}\mathscr{G} - \mathscr{F}^2} \, \mathrm{d}u \wedge \mathrm{d}t = g\kappa \, \mathrm{d}u \wedge \mathrm{d}t.$$

Particular details of the computations are in the proof of Lemma 1.　　　q.e.d.

Without any assumptions on the initial curve, we can bound the generated area from below by a linear function of time.

Corollary 1. *The Fenchel Theorem implies $A(\Sigma_t) \geqslant 2\pi t$ for all $t \in [0, \underline{t})$. Furthermore, when the curve is knotted on $[0, \underline{t})$, we get $A(\Sigma_t) \geqslant 4\pi t$ by the Milnor-Fáry Theorem* [29].

Lemma 8. *The evolution of the total torsion τ and the total generalized torsion ψ_3 of Γ_t during the framed curvature flow (1) is*

$$(13) \qquad \frac{\mathrm{d}}{\mathrm{d}t} \int_{\Gamma_t} \tau \, \mathrm{d}s = \frac{\mathrm{d}}{\mathrm{d}t} \int_{\Gamma_t} \psi_3 \, \mathrm{d}s = \int_{\Gamma_t} \psi_1 \psi_3 \kappa + \psi_2 \partial_s \kappa \, \mathrm{d}s.$$

Proof. Since Γ_t is closed, both integrals are equal, i.e.

$$\int_{\Gamma_t} \psi_3 \, \mathrm{d}s = \int_{\Gamma_t} \tau \, \mathrm{d}s + \int_{\Gamma_t} \partial_s \theta \, \mathrm{d}s = \int_{\Gamma_t} \tau \, \mathrm{d}s.$$

The right-hand side of (13) is obtained from (2) and (4).　　　q.e.d.

The estimates below are based a subset of the following *assumptions*:

I. There exists a fixed $\varepsilon > 0$ such that $|\theta| \leqslant \frac{\pi}{2} - \varepsilon$. In this case we define a constant $K_{\mathrm{I.}} := \cos\left(\frac{\pi}{2} - \varepsilon\right) > 0$ which will bound $\cos\theta$ from below.
II. The curvature κ is uniformly bounded from bellow by a constant $K_{\mathrm{II.}} > 0$, i.e. $\kappa(u, t) \geqslant K_{\mathrm{II.}}$ for all $t \in [0, \underline{t})$ and $u \in S^1$.

Note that assumption *I.* is also needed for the existence proof in Subsection 2.3 and follows from the assumptions given in Lemma 5, or alternatively Lemma 6. Assumption *II.*, on the other hand, can only be enforced up-to a time t away from the singularity $\underline{t}$, where the curvature blows up.

Proposition 4. *Let Γ_t be a solution to* (1). *If assumption* I. *holds, then*

$$(14) \qquad L(\Gamma_t) \leqslant \left(L^2(\Gamma_0) - 8\pi^2 K_{\mathrm{I.}} t\right)^{\frac{1}{2}}$$

and thus the terminal time can be bounded from above as

$$(15) \qquad \underline{t} \leqslant \left(8\pi^2 K_{\mathrm{I.}}\right)^{-1} L^2(\Gamma_0).$$

Moreover, assuming the curve is knotted on $[0, \underline{t})$, the $8\pi^2$ term in both (14) *and* (15) *estimates can be replaced by $32\pi^2$ as in Corollary* 1.

Proof. From assumption *I.* and the first part of Lemma 7 we have

$$\frac{\mathrm{d}}{\mathrm{d}t} L(\Gamma_t) = -\int_{\Gamma_t} \kappa^2 \cos\theta \; \mathrm{d}s \leqslant -K_{\mathrm{I.}} \int_{\Gamma_t} \kappa^2 \, \mathrm{d}s.$$

Using the Fenchel Theorem and Cauchy-Schwarz inequality, we obtain

$$\frac{\mathrm{d}}{\mathrm{d}t} L(\Gamma_t) \leqslant -\frac{K_{\mathrm{I.}}}{L(\Gamma_t)} \left(\int_{\Gamma_t} \kappa \, \mathrm{d}s\right)^2 \leqslant -\frac{4\pi^2 K_{\mathrm{I.}}}{L(\Gamma_t)}.$$

The result follows from the ODE comparison theorem.   q.e.d.

Proposition 5. *Let Γ_t be a solution to* (1) *and let Σ_t denote its associated trajectory surface. If assumptions* I. *and* II. *are satisfied, then we get*

$$A(\Sigma_t) \leqslant \frac{K_{\mathrm{II.}}}{12\pi^2 K_{\mathrm{I.}}} \left(L^3(\Gamma_0) - \left(L^2(\Gamma_0) - 8\pi^2 K_{\mathrm{I.}} t\right)^{\frac{3}{2}}\right).$$

Furthermore, as $\underline{t}$ is bounded by (15), *we get a global bound*

$$A(\Sigma_{\underline{t}}) \leqslant \frac{K_{\mathrm{II.}} L^3(\Gamma_0)}{12\pi^2 K_{\mathrm{I.}}}.$$

Proof. Assuming *I.* and *II.* and using Lemma 7 and Proposition 4 yields

$$\frac{\mathrm{d}}{\mathrm{d}t} A(\Sigma_t) \leqslant K_{\mathrm{II.}} L(\Gamma_t) \leqslant K_{\mathrm{II.}} \left(L^2(\Gamma_0) - 8\pi^2 K_{\mathrm{I.}} t\right)^{\frac{1}{2}}.$$

Integrating the inequality yields the result.   q.e.d.

3.2. Projected Area. In this subsection, we consider the following quantity

$$(16) \qquad A_p(\Gamma_t) := \frac{1}{2} \int_{\Gamma_t} \gamma \times \partial_s \gamma \, \mathrm{d}s = \frac{1}{2} \int_{S^1} \gamma \times \partial_u \gamma \, \mathrm{d}u$$

and use it to extend our area estimates for $\Sigma_{\underline{t}}$. The geometric interpretation of this quantity is revealed in following lemma.

Lemma 9. *For a given curve Γ_t, the quantity $A_p(\Gamma_t)$ defined in* (16) *is the largest algebraic area enclosed by any orthogonal projection of Γ_t.*

Proof. For any unit normal vector $\nu \in S^2$, let $\pi(\nu)$ be the projection operator onto $\{\nu\}^\perp$, i.e. $\pi(\nu) = \mathbb{I} - \nu \cdot \nu^T$, and let $\pi(\nu)\Gamma_t$ denote the projected planar curve paramerized by $\pi(\nu)\gamma$. Then

$$A(\pi(\nu)\Gamma_t) := \left\| \int_{S^1} \pi(\nu)\gamma \times \partial_u(\pi(\nu)\gamma) \, \mathrm{d}u \right\|$$

$$= \left\| A_p(\Gamma_t) - \int_{S^1} \langle \gamma, \nu \rangle \nu \times \partial_u \gamma \, \mathrm{d}u - \int_{S^1} \langle \partial_u \gamma, \nu \rangle \gamma \times \nu \, \mathrm{d}u \right\|$$

$$= \left\| A_p(\Gamma_t) + \nu \times \int_{S^1} \langle \partial_u \gamma, \nu \rangle \gamma - \langle \gamma, \nu \rangle \partial_u \gamma \, \mathrm{d}u \right\|,$$

where $A(\Gamma)$ denotes the algebraic area enclosed by a planar curve Γ. Double application of the triple vector product formula yields

$$A(\pi(\nu)\Gamma_t) = \| A_p(\Gamma_t) + \nu \times (\nu \times A_p(\Gamma_t)) \|$$

$$= \| A_p(\Gamma_t) + \langle A_p(\Gamma_t), \nu \rangle \nu - \|\nu\|^2 A_p(\Gamma_t) \|$$

$$= \| \langle A_p(\Gamma_t), \nu \rangle \nu \| = | \langle A_p(\Gamma_t), \nu \rangle |.$$

Thus, due to the Cauchy-Schwarz inequality, we have:

1. $A(\pi(\nu)\Gamma_t) \leqslant A_p(\Gamma_t)$ for all ν in S^2,
2. $A(\pi(A_p(\Gamma_t)^{-1} A_p(\Gamma_t))\Gamma_t) = A_p(\Gamma_t)$ when $A_p(\Gamma_t) > 0$.

The conjunction of 1. and 2. proves the statement. q.e.d.

Lemma 10. *The time derivative of $A_p(\Gamma_t)$ during* (1) *is*

$$(17) \qquad \frac{\mathrm{d}}{\mathrm{d}t} A_p(\Gamma_t) = -\int_{\Gamma_t} \kappa \beta_\theta \, \mathrm{d}s.$$

Proof. The derivation of this integral quantity is simplified because

$$\int_{\Gamma_t} \gamma \times \partial_s \gamma \, \mathrm{d}s = \int_{S^1} \gamma \times \partial_u \gamma \, \mathrm{d}u,$$

where $\mathrm{d}s = g \, \mathrm{d}u$ and, formally, $\partial_u = g\partial_s$. Thus we have

$$\frac{\mathrm{d}}{\mathrm{d}t} A_p(\Gamma_t) = \frac{1}{2} \int_{S^1} \partial_t \gamma \times \partial_u \gamma + \gamma \times \partial_u \partial_t \gamma \, \mathrm{d}u = \frac{1}{2} \int_{\Gamma_t} \kappa \nu_\theta \times T + \gamma \times \partial_s(\kappa \nu_\theta) \, \mathrm{d}s,$$

where $\nu_\theta \times T = -\beta_\theta$ and both parts of the integral yield the same value as

$$\int_{\Gamma_t} \gamma \times \partial_s(\kappa \nu_\theta) \, \mathrm{d}s = \int_{\Gamma_t} \partial_s(\gamma \times \kappa \nu_\theta) - T \times \kappa \nu_\theta \, \mathrm{d}s = -\int_{\Gamma_t} \kappa \beta_\theta \, \mathrm{d}s.$$

Adding these integrals leads to (17). q.e.d.

Proposition 6. *Let $\{(\Gamma_t, \theta_t)\}_{t \in [0, \underline{t})}$ develop a flat singularity at time $\underline{t}$, then*

$$A(\Sigma_{\underline{t}}) \geqslant \max_{t \in [0, \underline{t})} \|A_p(\Gamma_t)\|.$$

Proof. Let $x \in \mathbb{R}^3$ be the point to which the curve Γ_t shrinks towards as the time t approaches $\underline{t}$. Since $\Sigma_{\underline{t}} \cup \{x\}$ spans the initial curve Γ_0, its area must be at least that of minimal spanning surface, which has locally larger area that the projection. Formally, let dA' denote the area element of $\pi(\nu)\Gamma_t$, then

$$\mathscr{E}' = \|\partial_u \pi(\nu)\gamma\|^2 \leqslant \|\|\pi(\nu)\|\|^2 \|\partial_u \gamma\|^2 = g^2,$$
$$\mathscr{G}' = \|\partial_t \pi(\nu)\gamma\|^2 \leqslant \|\|\pi(\nu)\|\|^2 \|\partial_t \gamma\|^2 = \kappa^2.$$

With $\|\| \cdot \|\|$ being the spectral norm, $\|\|\pi(\nu)\|\| = \max(\sigma(\pi(\nu))) = 1$ and thus

$$dA' = \sqrt{\mathscr{E}'\mathscr{G}' - \mathscr{F}'^2}\, du \wedge dt \leqslant \sqrt{\mathscr{E}'\mathscr{G}'}\, du \wedge dt \leqslant g\kappa\, du \wedge dt = dA.$$

Note that the algebraic area of the projection is even smaller as the overlapping parts can annihilate.   q.e.d.

Proposition 7. *Let Γ_t be a solution to* (1) *and assume* I. *and* II., *then*

$$\frac{d}{dt}\|A_p(\Gamma_t)\| \leqslant 2K_{\mathrm{I.}} K_{\mathrm{II.}} L(\Gamma_t).$$

Proof. Applying the assumptions and Cauchy-Schwarz inequality yields

$$\frac{d}{dt}\|A_p(\Gamma_t)\| = \left\langle \frac{A_p(\Gamma_t)}{\|A_p(\Gamma_t)\|}, \frac{d}{dt} A_p(\Gamma_t) \right\rangle \leqslant \left\| \frac{d}{dt} A_p(\Gamma_t) \right\| \leqslant 2K_{\mathrm{I.}} K_{\mathrm{II.}} \left\| \int_{\Gamma_t} \beta_\theta\, ds \right\|.$$

The statement then follows from the fact that $\mathscr{R}_\theta$ is unitary.   q.e.d.

Since the area of any surface enclosed by the curve Γ_t is smaller than $\|A_p(\Gamma_t)\|$ (see proof of Proposition 6), the above proposition provides an upper bound on the growth of minimal spanning surface area.

Remark 5. *Note that for $\theta \equiv \frac{\pi}{2}$, both the length $L(\Gamma_t)$ and the projected area $A_p(\Gamma_t)$ remain constant during* (1), *as shown in* [**11**]. *On the other hand, for $\theta \equiv 0$ the motion is an L^2-gradient flow for the length functional (see* [**46**]*).*

3.3. Frame Topology. Let us consider the topology of the moving θ-frame and its possible ramifications on the long-term behaviour of the framed curvature flow. We do so by analysing the time evolution of two geometric quantities, named writhe and twist, which are closely connected to the topology of the moving frame. Writhe of an embedded curve is an averaged sum of all signed crossings over the space of all orthogonal projections, but can also be written using Gauss formula as

$$\mathrm{W_r}(\Gamma_t) = \frac{1}{4\pi} \iint\limits_{\Gamma_t \times \Gamma_t} \frac{\langle \gamma(s,t) - \gamma(s',t), T(s,t) \times T(s',t) \rangle}{\|\gamma(s,t) - \gamma(s',t)\|^3}\, ds \wedge ds'.$$

The second important geometric quantity describing the frame topology is the total twist of the θ-frame, which reads

$$
\begin{aligned}
\mathrm{T}_{\mathrm{w}}^{\theta}(\Gamma_t) &= \frac{1}{2\pi} \int_{\Gamma_t} \langle \nu_\theta \times \partial_s \nu_\theta, T \rangle \, \mathrm{d}s \\
&= \frac{1}{2\pi} \int_{\Gamma_t} -\psi_1 \langle \nu_\theta \times T, T \rangle + \psi_3 \langle \nu_\theta \times \beta_\theta, T \rangle \, \mathrm{d}s \\
&= \frac{1}{2\pi} \int_{\Gamma_t} \psi_3 \, \mathrm{d}s = \mathrm{T}_{\mathrm{w}}^{F}(\Gamma_t) + \frac{1}{2\pi} \deg(\theta_t),
\end{aligned}
$$

where $\deg(\theta_t)$ is the topological degree of $\theta_t \colon S^1 \to S^1$ and $\mathrm{T}_{\mathrm{w}}^{F}(\Gamma_t)$ is the normalized total twist (i.e. total twist assiciated with the Frenet frame):

$$
\mathrm{T}_{\mathrm{w}}^{F}(\Gamma_t) = \frac{1}{2\pi} \int_{\Gamma_t} \tau \, \mathrm{d}s.
$$

The writhe and twist are connected via the Călugăreanu–White–Fuller Theorem [**23**, **82**] which states that

$$
\text{(18)} \qquad\qquad \mathrm{S}_{\mathrm{Lk}}^{\bullet}(\Gamma_t) = \mathrm{W}_{\mathrm{r}}(\Gamma_t) + \mathrm{T}_{\mathrm{w}}^{\bullet}(\Gamma_t),
$$

where $\bullet$ represents either F or θ and $\mathrm{S}_{\mathrm{Lk}}^{\theta}(\Gamma_t)$, $\mathrm{S}_{\mathrm{Lk}}^{F}(\Gamma_t)$ are the self-linking numbers for the Frenet frame and the θ-frame, respectively. With the help of this theorem we can describe the evolution of writhe for embedded curves.

Proposition 8. *Let $\{(\Gamma_t, \theta_t)\}_{t\in[0,\underline{t})}$ be a solution to (1). Consider $t \in [0, \underline{t})$ such that $\Gamma_t \hookrightarrow \mathbb{R}^3$ (i.e. Γ_t is embedded) and $\kappa(u,t) > 0$ for all $u \in S^1$. Then*

$$
\text{(19)} \qquad\qquad \frac{\mathrm{d}}{\mathrm{d}t} \mathrm{W}_{\mathrm{r}}(\Gamma_t) = -\frac{1}{2\pi} \int_{\Gamma_t} \psi_1 \psi_3 \kappa + \psi_2 \partial_s \kappa \, \mathrm{d}s.
$$

Proof. The assumptions imply that the time derivative of $\mathrm{S}_{\mathrm{Lk}}^{F}(\Gamma_t)$ exists and is equal to 0. Thus, we may differentiate (18) to obtain

$$
\frac{\mathrm{d}}{\mathrm{d}t} \mathrm{W}_{\mathrm{r}}(\Gamma_t) = \frac{\mathrm{d}}{\mathrm{d}t} \left[\mathrm{S}_{\mathrm{Lk}}^{F}(\Gamma_t) - \mathrm{T}_{\mathrm{w}}^{F}(\Gamma_t) \right] = -\frac{1}{2\pi} \frac{\mathrm{d}}{\mathrm{d}t} \int_{\Gamma_t} \tau \, \mathrm{d}s.
$$

The formula (19) then follows from Lemma 8.   q.e.d.

Remark 6. *Note that since ν_θ is continuous, the degree of θ cannot change during the flow and the difference $\mathrm{S}_{\mathrm{Lk}}^{\theta}(\Gamma_t) - \mathrm{S}_{\mathrm{Lk}}^{F}(\Gamma_t)$ is a constant integer.*

The following proposition provides a necessary topological condition needed to close the trajectory surface in sense of ending the flow in a flat singularity described in Subsection 2.4.

Proposition 9. *Assume that $\{(\Gamma_t, \theta_t)\}_{t\in[0,\underline{t})}$ develops a flat singularity and (Γ_0, θ_0) is not a Seifert framing. Then there must exist $t \in [0, \underline{t})$ such that either $\kappa(u,t) = 0$ at some point $u \in S^1$ or Γ_t is not embedded.*

Proof. The Seifert framing must have zero self-linking number [**80**].   q.e.d.

4. Generated Surfaces

By adjusting the definition of the θ-velocity, the framed curvature flow can be formulated such that its associated trajectory surface has various interesting properties. These specific formulations are explored in this section. We consider trajectory surfaces of constant mean curvature in Subsection 4.1 and then constant Gaussian curvature in Subsection 4.2. Other special surfaces, such as surfaces of constant ratio of principle curvatures, proposed in [53], fall outside the scope of this manuscript and may be the subject of future work.

4.1. Constant Mean Curvature. In this subsection, we consider the use of framed curvature flow as a means of solving the Björling problem for minimal surfaces and its generalisation for non-minimal surfaces of constant mean curvature (see [20]).

Proposition 10. *For a fixed constant $H \in \mathbb{R}$, consider the framed curvature flow* (1) *with the θ-velocity given by*

$$(20) \qquad v_\theta = \kappa H - (\kappa \partial_s \psi_3 + 2 \partial_s \kappa \psi_3) \kappa^{-2} \psi_1 + (\kappa^3 + \kappa \psi_3^2 - \partial_s^2 \kappa) \kappa^{-2} \psi_2.$$

The trajectory surface $\Sigma_{\underline{t}}$ generated by this flow has a constant mean curvature equal to the prescribed value H.

Proof. Substitution of (20) to Lemma 1. q.e.d.

The following results are all related to the Flux theorem introduced in [49, 50].

Proposition 11 (Flux Theorem). *Let $\{(\Gamma_t, \theta_t)\}_{t \in [0,\underline{t})}$ be a solution to the framed curvature flow with θ-velocity defined in* (20). *Then for any $a \in \mathbb{R}^3$*

$$(21) \qquad H \int_{\partial \Sigma_t} \langle \gamma \times T, a \rangle \, \mathrm{d}s + \int_{\partial \Sigma_t} \langle \nu_\theta, a \rangle \, \mathrm{d}s = 0,$$

where $\partial \Sigma_t = \Gamma_0 \cup \Gamma_t$ is the boundary of the associated trajectory surface Σ_t.

Proof. Multiple proofs can be found in e.g. [54], where the unit conormal vector from Theorem 5.1.1. is equivalent to the θ-normal ν_θ. q.e.d.

Combining the Flux theorem with the evolution equations for the projected area A_p leads to a simple formula for the derivative of total θ-normal.

Corollary 2. *If $\{(\Gamma_t, \theta_t)\}_{t \in [0,\underline{t})}$ is a solution to* (1) *with v_θ from* (20), *then*

$$\frac{\mathrm{d}}{\mathrm{d}t} \int_{\Gamma_t} \nu_\theta \, \mathrm{d}s = 2H \int_{\Gamma_t} \kappa \beta_\theta \, \mathrm{d}s.$$

Proof. The boundary $\partial \Sigma_t$ consists of Γ_t and Γ_0, but the former is static. Differentiation of the Flux theorem (21) thus leads to

$$(22) \qquad H \frac{\mathrm{d}}{\mathrm{d}t} \int_{\Gamma_t} \gamma \times T \, \mathrm{d}s + \frac{\mathrm{d}}{\mathrm{d}t} \int_{\Gamma_t} \nu_\theta \, \mathrm{d}s = 0.$$

The result is then obtained by rearranging (22) and using Lemma 10. q.e.d.

The Flux theorem enables the following necessary conditions for flat singularity formation during the flow that generates surfaces of constant mean curvature.

Corollary 3. *When $\{(\Gamma_t, \theta_t)\}_{t \in [0, \underline{t})}$ develops a flat singularity at the terminal time $\underline{t}$, the surface $\Sigma_{\underline{t}}$ only has one non-trivial boundary Γ_t, and thus*

$$A_p(\Gamma_0) = -\frac{1}{H} \int_{\Gamma_0} \nu_\theta \, \mathrm{d}s$$

Corollary 4. *Assume that $\{(\Gamma_t, \theta_t)\}_{t \in [0, \underline{t})}$ solves the framed curvature flow with υ_θ from (20) and develops a flat singularity. Then*

$$L(\Gamma_0) \geqslant 2H \|A_p(\Gamma_0)\|.$$

In particular, if Γ_0 is simple planar curve enclosing area A, then

$$L(\Gamma_0) \geqslant 2HA.$$

Proof. For any unit vector $a \in S^2$, we have $2H|\langle A_p(\Gamma_0), a \rangle| \leqslant L(\Gamma_0)$ from Corollary 5.1.7 of [**54**]. q.e.d.

Important subclass of surfaces with constant mean curvature are the minimal surfaces [**59**, **73**] characterised by $H = 0$. In nature, minimal surfaces emerge in the context of soap films [**34**, **35**], cell membranes [**51**], crystallographic structure of zeolites [**6**, **7**, **78**] and as the apparent horizon of a black hole [**41**].

For the case of minimal surfaces, many of the previous results derived from the Flux theorem significantly simplify. Additionally, when the flow develops a flat singularity, the associated trajectory surface effectively represents a valid solution to the Plateau problem with single boundary curve Γ_0.

Corollary 5 (Corollary 5.1.5 from [**54**]). *For minimal surfaces with $H = 0$, we have even stricter conditions, namely for all $a \in \mathbb{R}^3$*

$$\int_{\partial \Sigma_t} \langle \nu_\theta, a \rangle \, \mathrm{d}s = 0, \qquad\qquad \int_{\partial \Sigma_t} \langle \nu_\theta, \gamma \times a \rangle \, \mathrm{d}s = 0.$$

We end this subsection with analysis of specific examples of solutions to (20) with simple initial configurations. First example illustrates the configuration that leads to the simplest minimal surface, which is a subset of the flat plane.

Example 5. *Let the initial curve Γ_0 be a closed convex planar curve and $\theta_0 \equiv 0$. Then the framed curvature flow with θ-velocity from (20) and $H = 0$ is equivalent to the curve shortening flow and generates a flat surface $\Sigma_{\underline{t}}$ equivalent to the convex hull of Γ_0 in a finite time $\underline{t}$ when the Γ_t shrinks down to a round point (see [**31**, **37**]).*

More analytical examples can be obtained by considering configurations with helical and cylindrical symmetries.

Example 6 (Helical symmetry). *For a constant θ_0 consider evolving helix*

$$\gamma_0(u) := \begin{bmatrix} \varrho_0 \cos u \\ \varrho_0 \sin u \\ wu \end{bmatrix}, \qquad\qquad \gamma(t, u) := \begin{bmatrix} \varrho(t) \cos(u + \upsilon(t)) \\ \varrho(t) \sin(u + \upsilon(t)) \\ wu + \omega(t) \end{bmatrix},$$

where ρ_0 and w are positive constants and ρ, v, ω are functions of time t. Since $\kappa = \varrho g^{-2}$ and $\tau = w g^{-2}$, the problem (20) reduces to the following system

$$(23) \qquad \frac{\mathrm{d}}{\mathrm{d}t} \begin{bmatrix} \theta \\ \varrho \\ \omega \\ v \end{bmatrix} = \frac{1}{g^3} \begin{bmatrix} g \sin\theta + \rho g H \\ -g\rho\cos\theta \\ \rho^2 \sin\theta \\ -w\sin\theta \end{bmatrix}, \qquad \begin{bmatrix} \theta \\ \varrho \\ \omega \\ v \end{bmatrix}\Bigg|_{t=0} = \begin{bmatrix} \theta_0 \\ \varrho_0 \\ 0 \\ 0 \end{bmatrix},$$

where $g^2 = \varrho^2 + w^2$. Similar helicoidal surfaces of constant mean curvature were studied in e.g. [39].

Considering cylindrically symmetrical configurations leads to the family of Delaneu surfaces, first classified in [26].

Example 7 (Cylindrical symmetry). *Setting $w = 0$ reduces (23) to*

$$\frac{\mathrm{d}}{\mathrm{d}t} \begin{bmatrix} \theta \\ \varrho \\ \omega \end{bmatrix} = \frac{1}{\varrho^2} \begin{bmatrix} \sin\theta + \varrho H \\ -\varrho\cos\theta \\ \varrho\sin\theta \end{bmatrix}, \qquad \begin{bmatrix} \theta \\ \varrho \\ \omega \end{bmatrix}\Bigg|_{t=0} = \begin{bmatrix} \theta_0 \\ \varrho_0 \\ 0 \end{bmatrix}.$$

4.2. Constant Gaussian Curvature. Unlike the mean curvature flow or the minimal surface generating flow [64], the framed curvature flow can be used for generating developable surfaces or surfaces of any prescribed Gaussian curvature.

Proposition 12. *For a fixed constant $K \in \mathbb{R}$, consider a framed curvature flow (1) with the θ-velocity given by*

$$(24a) \qquad v_\theta = -\kappa\psi_2^{-1}K - (\kappa\partial_s\psi_3 + 2\partial_s\kappa\psi_3)\kappa^{-2}\psi_1$$

$$(24b) \qquad - \kappa\psi_2^{-1}\psi_3^2 - (\partial_s^2\kappa - \kappa\psi_3^2)\kappa^{-2}\psi_2.$$

The trajectory surface $\Sigma_{\underline{t}}$ generated by this flow has a constant Gaussian curvature equal to the prescribed value K.

Proof. Substitution of (24) to Lemma 1.   q.e.d.

Important examples of surfaces with constant Gaussian curvature are developable surfaces. For this specific case, the Gauss-Bonnet formula significantly simplifies and can be used to uncover an unexpected integral of motion.

Proposition 13. *Let $\{(\Gamma_t, \theta_t)\}_{t\in[0,\underline{t})}$ be a solution to the framed curvature flow with θ-velocity defined in (24) with K set to 0. Then the integral of ψ_1 over the curve Γ_t at any time $t \in [0,\underline{t})$ is preserved.*

Proof. The Gauss-Bonnet theorem states that

$$(25) \qquad \int_{\Sigma_t} K \, \mathrm{d}A + \int_{\partial\Sigma_t} \kappa_g \, \mathrm{d}s = 2\pi\chi(\Sigma_t),$$

where $\mathrm{d}A = \kappa g \, \mathrm{d}u \wedge \mathrm{d}t$ (see proof of Proposition 6), κ_g is the geodesic curvature at the boundary $\partial\Sigma_t = \Gamma_0 \cup \Gamma_t$ and $\chi(\Sigma_t) = 0$ is the Euler characteristic of an annulus. Differentiation of (25) and subsequent substitution yields

$$\frac{\mathrm{d}}{\mathrm{d}t} \int_{\Gamma_t} \psi_1 \, \mathrm{d}s = -\int_{\Gamma_t} \kappa K \, \mathrm{d}s,$$

where ψ_1 is the geodesic curvature of Γ_t on Σ_t and the integrand on the right hand side is 0 by the assumption that $K = 0$.   q.e.d.

As in the previous subsection, we construct analytical examples using configurations with helical and cylindrical symmetries.

Example 8 (Helical symmetry). *For a constant θ_0 consider evolving helix*

$$\gamma_0(u) := \begin{bmatrix} \varrho_0 \cos u \\ \varrho_0 \sin u \\ wu \end{bmatrix}, \qquad \gamma(t, u) := \begin{bmatrix} \varrho(t) \cos(u + v(t)) \\ \varrho(t) \sin(u + v(t)) \\ wu + \omega(t) \end{bmatrix},$$

where ρ_0 and w are positive constants and ρ, v, ω are functions of time t. Since $\kappa = \varrho g^{-2}$ and $\tau = w g^{-2}$, the problem (24) reduces to the following system

$$(26) \qquad \frac{\mathrm{d}}{\mathrm{d}t} \begin{bmatrix} \theta \\ \varrho \\ \omega \\ v \end{bmatrix} = \frac{1}{g^3} \begin{bmatrix} \frac{Kg^4 + w^2 \cos^2 \theta}{g \sin \theta} \\ -g\rho \cos \theta \\ \rho^2 \sin \theta \\ -w \sin \theta \end{bmatrix}, \qquad \begin{bmatrix} \theta \\ \varrho \\ \omega \\ v \end{bmatrix}\Bigg|_{t=0} = \begin{bmatrix} \theta_0 \\ \varrho_0 \\ 0 \\ 0 \end{bmatrix},$$

where $g^2 = \varrho^2 + w^2$. This solution leads to a family of helical trajectory surfaces of constant Gaussian curvature.

Example 9 (Cylindrical symmetry). *Setting $w = 0$ reduces (26) to*

$$\frac{\mathrm{d}}{\mathrm{d}t} \begin{bmatrix} \theta \\ \varrho \\ \omega \end{bmatrix} = \frac{1}{\varrho^2} \begin{bmatrix} (\sin \theta)^{-1} Kg^3 \\ -\varrho \cos \theta \\ \varrho \sin \theta \end{bmatrix}, \qquad \begin{bmatrix} \theta \\ \varrho \\ \omega \end{bmatrix}\Bigg|_{t=0} = \begin{bmatrix} \theta_0 \\ \varrho_0 \\ 0 \end{bmatrix}.$$

5. Conclusion

The framed curvature flow offers a promising extension of classical curvature-driven geometric flows of space curves, providing a rich configuration space of motion laws with potential applications in the analysis of surfaces with prescribed curvature and beyond.

In this work, we introduced the framed curvature flow as a generalization of the curve shortening flow and vortex filament equation, incorporating a time-dependent moving frame to govern the direction of curvature-driven motion. We established local existence and uniqueness for a simplified version of this flow, derived global estimates for key geometric and topological quantities, and examined the trajectory surfaces produced by variations of the flow, including those leading to surfaces of constant mean or Gaussian curvature. Additionally, we classified singularities that may arise during the flow.

More research is needed to explore local existence across a broader range of θ-velocity settings. Future work could also investigate motion laws that generate other surface types, such as those with a constant principal curvature ratio [53], or surfaces that minimize energies like Willmore energy [79] or various repulsive energies [84, 85].

Another direction for future research could involve extending the concept of framed curvature flow to higher-dimensional spaces with more than one codimension, and exploring possible connections between the generated trajectory varieties and Open book decomposition.

Further insights may be gained through rigorous numerical analysis and experiments with different θ-velocity settings. Finally, the examples of singularities involving curvature blow-up, discussed in Subsection 2.4, should be expanded and studied in greater detail.

References

[1] N. H. Abdel-All, R. A. Hussien and T. Youssef, *Hasimoto Surfaces*, Life Science Journal, **9** (2012), 556–560.

[2] A. Abrams, J. H. Cantarella, J. H. G. Fu, M. Ghomi and R. Howard, *Circles minimize most knot energies*, Topology, **42** (2001), 381–394.

[3] U. Abresch and J. Langer, *The normalized curve shortening flow and homothetic solutions*, J. Differential Geom. **23(2)** (1986), 175–196.

[4] S. J. Altschuler, *Singularities for the curve shortening flow for space curves*, J. Differential Geom., **34** (1991), 491–514.

[5] S. J. Altschuler and M. A. Grayson, *Shortening space curves and flow through singularities*, J. Differential Geom., **35** (1992), 283–298.

[6] S. Andersson, S. T. Hyde and J. O. Bovin, *On the periodic minimal surfaces and the conductivity mechanism of α-AgI*, Zeitschrift für Kristallographie, **173** (1985), 97–99.

[7] S. Andersson, S. T. Hyde, K. Larsson and S. Lidin, *Minimal Surfaces and Structures: From Inorganic and Metal Crystals to Cell Membranes and Biopolymers*, Chemical Reviews, **88** (1988), 221–242.

[8] B. Andrews, *Singularities in crystalline curvature flows*, Asian J. Math., **6** (2002), 101–122.

[9] S. Angenent, *Parabolic equations for curves on surfaces. I: Curves with p-integrable curvature*, Ann. Math., **132(2)** (1990), 451–483.

[10] S. Angenent, *Nonlinear analytic semi-flows*, Proc. R. Soc. Edinb., Sect. A, **115** (1990), 91–107.

[11] R. J. Arms and F. R. Hama, *Localized Induction Concept on a Curved Vortex and Motion of an Elliptic Vortex Ring*, Physics of Fluids, **8** (1965), 553–559.

[12] I. Bakas and C. Sourdis, *Dirichlet sigma models and mean curvature flow*, Journal of High Energy Physics 2007, **6** (2007), 057.

[13] R. Bamler and B. Kleiner, *Ricci flow and diffeomorphism groups of 3-manifolds*, Journal of the American Mathematical Society, **36(1)** (2022).

[14] C. F. Barenghi, D. C. Samuels, G. H. Bauer and R. J. Donnelly, *Superfluid vortex lines in a model of turbulent flow*, Physics of Fluids, **9** (1997), 2631–2643.

[15] S. Bartels and P. Reiter, *Numerical solution of a bending-torsion model for elastic rods*, Numerische Mathematik, **146** (2020), 661–697.

[16] M. Beneš, M. Kolář and D. Ševčovič, *Qualitative and Numerical Aspects of a Motion of a Family of Interacting Curves in Space*, SIAM Journal on Applied Mathematics, **82** (2022).

[17] M. Bergou, M. Wardetzky, S. Robinson, B. Audoly and E. Grinspun, *Discrete elastic rods*, ACM SIGGRAPH, **63** (2008).

[18] R. L. Bishop, *There is More than One Way to Frame a Curve*, Amer. Math. Monthly, **82(3)** (1975), 246–251.

[19] S. Blatt, *The Gradient Flow of O'Hara's Knot Energies*, Mathematische Annalen, **370** (2018), 993–1061.

[20] D. Brander, J. F. Dorfmeister, *The Björling problem for non-minimal constant mean curvature surfaces*, Comm. Anal. Geom., **18** (2010), 171–194.

[21] K. Brazda, L. Lussardi and U. Stefanelli, *Existence of varifold minimizers for the multiphase Canham–Helfrich functional*, Calc. Var., **59** (2020), 93.

[22] S. Brendle and R. Schoen, *Manifolds with 1/4-pinched curvature are space forms*, J. Amer. Math. Soc., **22** (2009), 287—307.

[23] G. Călugăreanu, *Sur les classes d'isotopie des noeuds tridimensionels et leurs invariants*, Czech. Math. J., **11** (1961), 588–625.

[24] B. Chopard and M. Droz, *Cellular automata modeling of physical systems*, Collection AléaSaclay: Monographs and Texts in Statistical Physics. Cambridge University Press, Cambridge, 1998.

[25] K. Corrales, Non existence of type II singularities for embedded and unknotted space curves, preprint, arXiv:1605.03100v1, 2016.

[26] Ch. Delaunay, Sur la surface de révolution dont la courbure moyenne est constante, *Journal de Mathématiques Pure et Appliquée* **16** (1841), 309–321.

[27] E. Demainea and J. O'Rourke, *Geometric folding algorithms. Linkages, origami, polyhedra*, Cambridge Univ. Press, Cambridge, 2007.

[28] L. C. Evans, *Partial differential equations*, Second ed., Graduate Studies in Mathematics, vol. 19, American Mathematical Society, Providence, RI, 2010.

[29] I. Fáry, *Sur la courbure totale d'une courbe gauche faisant un noeud*, Bulletin de la Société Mathématique de France, **77** (1949), 128–138.

[30] D. Fuchs and S. Tabachnikov, *More on paperfolding*, Amer. Math. Monthly, **106** (1999), 27-–35.

[31] M. Gage and R. S. Hamilton, *The heat equation shrinking convex plane curves*, *J. Differential Geom.*, **1** (1986), 69–96.

[32] M. Ghomi, Classical open problems in differential geometry, 2019.

[33] Y. Giga and N. Požár, *A level set crystalline mean curvature flow of surfaces*, Adv. Differential Equations, *21*, 631-698.

[34] R. E. Goldsteina, H. K. Moffatt, A. I. Pescia and R. L. Ricca, *Soap-film Möbius strip changes topology with a twist singularity*, Proceedings of the National Academy of Sciences of the United States of America, **107** (2010), 21979–21984.

[35] R. E. Goldstein, J. McTavish, H. K. Moffatt and A. I. Pesci, *Boundary singularities produced by the motion of soap films*, Proceedings of the National Academy of Sciences of the United States of America, **111** (2014), 8339–8344.

[36] T. Gotō, *Relativistic Quantum Mechanics of One-Dimensional Mechanical Continuum and Subsidiary Condition of Dual Resonance Model*, Progress of Theoretical Physics, *46(5)* (1971), 1560-–1569.

[37] M. Grayson, *The heat equation shrinks embedded plane curves to round points*, J. Differential Geom., **(26)** (1987), 285–314.

[38] J. O'Hara, *Energy functionals of knots*, In Topology Hawaii (Honolulu, HI, 1990), 201-–214. World Sci. Publ., River Edge, NJ, 1992.

[39] Y. Hatakeyama and M. Koiso, Stability of helicoidal surfaces with constant mean curvature, *International Journal of Mathematics for Industry* **12** (2020).

[40] T. Y. Hou, J. Lowengrub, and M. Shelley, *Removing the stiffness from interfacial flows and surface tension*, J. Comput. Phys., **114** (1994), 312–338.

[41] G. Huisken and T. Ilmanen, *The inverse mean curvature flow and the Riemannian Penrose inequality*, J. Differential Geom., **59** (3), 2001, 353–437.

[42] R. A. Hussien and S. G. Mohamed, *Generated Surfaces via Inextensible Flows of Curves in* $\mathbb{R}^3$, Journal of Applied Mathematics, **2016** (2016), 1–8.

[43] T. Ishiwata and S. Yazaki, *On the blow-up rate for fast blow-up solutions arising in an anisotropic crystalline motion*, Journal of Computational and Applied Mathematics, **159(1)** (2003), 55–64.

[44] J. P. Keener, *The dynamics of three-dimensional scroll waves in excitable media*, Physica D, **31** (1988), 269–276.

[45] G. Khan, A condition ensuring spatial curves develop type-II singularities under curve shortening flow, preprint, arXiv:1209.4072v3, 2015.

[46] M. Kimura, *Geometry of hypersyrfaces and moving hypersurfaces in Rm for the study of moving boundary problems*, Topics on partial differential equations, Jindřich Nečas Center for Mathematical Modeling Lecture notes, **4(2)** (2008), 39-–93.

[47] M. Kimura, *Numerical analysis for moving boundary problems using the boundary tracking method*, Jpn. J. Indust. Appl. Math., **14** (1997), 373–398.

[48] M. Kolář, M. Beneš, J. Kratochvíl, P. Pauš, *Modeling of Double Cross-Slip by Means of Geodesic Curvature Driven Flow*, Acta Physica Polonica Series A, **134(3)** (2018), 667–670.

[49] R. Kusner, Global Geometry of Extremal Surfaces in Three-Space, *Thesis (doctoral) - University of California, Berkeley* (1987).

[50] R. Kusner, Bubbles, conservation laws, and balanced diagrams, *Math. Sci. Res. Inst. Publ., Springer, New York* **17** (1991), 103–108.

[51] M. Larsson and K. Larsson, *Periodic minimal surface organizations of the lipid bilayer at the lung surface and in cubic cytomembrane assemblies*, Advances in Colloid and Interface Science, **205** (2014), 68–73.

[52] F. Litzinger, *Singularities of low entropy high codimension curve shortening flow*, arXiv (2023), arXiv:math/2304.02487.

[53] Y. Liu, O. Pirahmad, H. Wang, D. L. Michels, H. Pottmann, On Helical Surfaces with a Constant Ratio of Principal Curvatures arXiv (2022), https://doi.org/10.48550/arXiv.2204.06443.

[54] R. López, *Constant Mean Curvature Surfaces with Boundary*, Springer Monographs in Mathematics (SMM), 2013.

[55] A. Lunardi, *Abstract quasilinear parabolic equations*, Math. Ann., **267** (1984), 395–416.

[56] T. Machon, H. Aharoni, Y. Hu and R. D. Kamien, *Aspects of Defect Topology in Smectic Liquid Crystals*, Commun. Math. Phys. **372** (2019), 525–542.

[57] F. C. Marques and A. Neves, *Min-Max theory and the Willmore conjecture*, Annals of Mathematics, **179** (2014), 683–782.

[58] F. Maucher and P. Sutcliffe, *Untangling Knots Via Reaction-Diffusion Dynamics of Vortex Strings*, Physical Review Letters, **116** (2016), 178101.

[59] W. H. Meeks III and J. Pérez, *A Survey on Classical Minimal Surface Theory*, University Lecture Series, **60** (2012), 182.

[60] K. Mikula and D. Ševčovič, *Evolution of plane curves driven by a nonlinear function of curvature and anisotropy*, SIAM J. Appl. Math., **61** (2001), 1473–1501.

[61] K. Mikula and J. Urbán, *A new tangentially stabilized 3D curve evolution algorithm and its application in virtual colonoscopy*, Adv. Comput. Math., **40** (2014), 819–837.

[62] J. Minarčík and M. Beneš, *Long-term behavior of curve shortening flow in $\mathbb{R}^3$*, SIAM J. Math. Anal., **52** (2020), 1221–1231.

[63] J. Minarčík and M. Beneš, *Nondegenerate Homotopy and Geometric Flows*, Homology, Homotopy and Applications, **24** (2022), 255—264.

[64] J. Minarčík and M. Beneš, *Minimal surface generating flow for space curves of non vanishing torsion*, Discrete Contin. Dyn. Syst. Ser. B, **27** (2022), 6605—6617.

[65] T. Mura, *Micromechanics of Defects in Solids*, Springer Netherlands, 1987.

[66] J. Nambu, *Quark model and the factorization of the Veneziano amplitude*, Broken Symmetry, (1995), 258–267.

[67] P. J. Olver, *Invariant submanifold flows*, Journal of Physics A: Mathematical and Theoretical, **41** (2008), 344017.

[68] S. Osher and J. A. Sethian, *Fronts Propagating with Curvature Dependent speed: Algorithms Based on Hamilton-Jacobi Formulation*, Journal of Computational Physics, **79** (1988), 12–49.

[69] M. Padilla, A. Chern, F. Knöppel, U. Pinkall and P. Schröder, *On Bubble Rings and Ink Chandeliers*, ACM Trans. Graph., **38** (2019), 1–14.

[70] M. Padilla, O. Gross, F. Knöppel, A. Chern, U. Pinkall and P. Schröder, *Filament based plasma*, ACM Trans. Graph., **41** (2022), 1–14.

[71] G. Perelman, *The entropy formula for the Ricci flow and its geometric applications*, arXiv (2002), arXiv:math/0211159.

[72] G. Perelman, *Ricci flow with surgery on three-manifolds*, arXiv (2003), arXiv:math/0303109.

[73] J. Pérez, *A New Golden Age of Minimal Surfaces*, Notices of the American Mathematical Society, **64(04)** (2016).

[74] G. Da Prato and P. Grisvard, *Equations d'évolution abstraites non linéaires de type parabolique*, Ann. Mat. Pura Appl., **4** (1979), 329–396.

[75] M. Remešíková, K. Mikula, P. Sarkoci, and D. Ševčovič, *Manifold evolution with tangential redistribution of points*, SIAM J. Sci. Comput., **36(4)** (2014), A1384–A1414.

[76] R. L. Ricca, *Rediscovery of Da Rios equations*, Nature, **352** (1991), 561–562.

[77] G. Sapiro, *Geometric partial differential equations and image analysis*, Cambridge University Press, Cambridge, 2001.

[78] L. E. Scriven, *Equilibrium bicontinuous structure*, Nature, **263** (1976), 123–125.

[79] Y. Soliman, A. Chern, O. Diamanti, F. Kn oppel, U. Pinkall, and P. Schr oder, *Constrained Willmore surfaces*, ACM Trans. Graph., **40** (2021), 1–17.

[80] D. W. L. Sumners, I. Cruz-White and R. L. Ricca, *Zero helicity of Seifert framed defects*, J. Phys. A., **54** (2021), 295203.

[81] L. Vega, *The dynamics of vortex filaments with corners*, Communications on Pure and Applied Analysis, **14(4)** (2015), 1581–1601.

[82] J. H. White, *Self-linking and the Gauss integral in higher dimensions*, Am. J. Math., **91** (1969), 693–728.

[83] A. R. Yeates, G. Hornig, and A. L. Wilmot-Smith, *Topological constraints on magnetic relaxation*, Phys. Rev. Lett., **105** (2010), 085002.

[84] C. Yu, C. Brakensiek, H. Schumacher and K. Crane, *Repulsive Surfaces*, ACM Trans. Graph., **40** (2021).

[85] C. Yu, H. Schumacher and K. Crane, *Repulsive Curves*, ACM Trans. Graph., **40** (2021).

[86] S. Zhong, Z. Zhao, X. Wan, *Geometry of solutions of the geometric curve flows in space.*, Authorea (2022), DOI: 10.22541/au.166756688.88270742/v1.

[87] S. Zuccher and R. L. Ricca, *Creation of quantum knots and links driven by minimal surfaces*, Journal of Fluid Mechanics, **942** (2022).